IN VIVO SUBJECT-SPECIFIC ESTIMATION OF CERVICAL SPINE DISC MATERIAL PROPERTIES

Dongge Jia[1], Soumaya Ouhsousou[1], Clarissa M. LeVasseur[2], Jeremy Shaw[3], William Anderst[2], and John C. Brigham[1]

[1] Department of Civil and Environmental Engineering, University of Pittsburgh
[2] Department of Orthopaedic Surgery, University of Pittsburgh
[3] Department of Orthopaedic Surgery, University of Pittsburgh Medical Center

Background & Motivation

- ~150,000 arthrodesis surgeries in 2020 – 25% are expected to require a 2nd surgery due to adjacent segment disease (ASD).
- There is debate whether ASD is caused by excessive motion and disc loading or other patient-specific factors.

- A subject-specific computational spine model could help evaluate intervertebral disc degeneration.
- **No previously developed spine model has been thoroughly validated with *in vivo* behavior**, and instead often only use cadaver models.

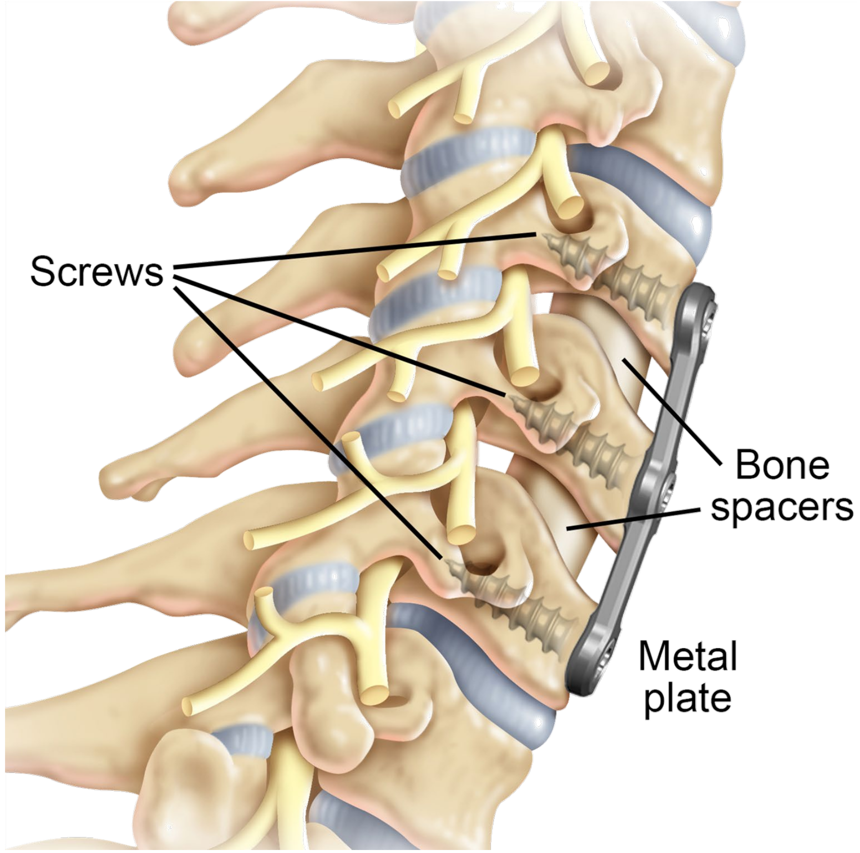

Cervical fusion. *Degenerated intervertebral discs are replaced by bone spacers and a fusion plate is added to stabilize the spine. The intervertebral disc above and below the fusion are susceptible to degenerative changes after fusion.*

Image Source: https://www.cervicaldisc.com/Portals/0/Fusion_1.jpg

Research Objective

The **overall objective** of this work is to identify biomechanical markers/factors that indicate the potential for cervical spine disc degeneration, particularly following spinal fusion surgery.

The **current technical objective** is to establish a consistent approach to create subject-specific cervical spine computational models, including non-invasively estimated *in vivo* subject-specific material properties of each disc, using *in vivo* motion trials of a patient with disc degeneration.

- Establish a numerical modeling approach, particularly the required components, to accurately simulate the kinematic response of subject-specific cervical spine.
- Estimate subject-specific disc material properties based on *in vivo* kinematics data.

Cervical Vertebrae Geometry from Imaging Data

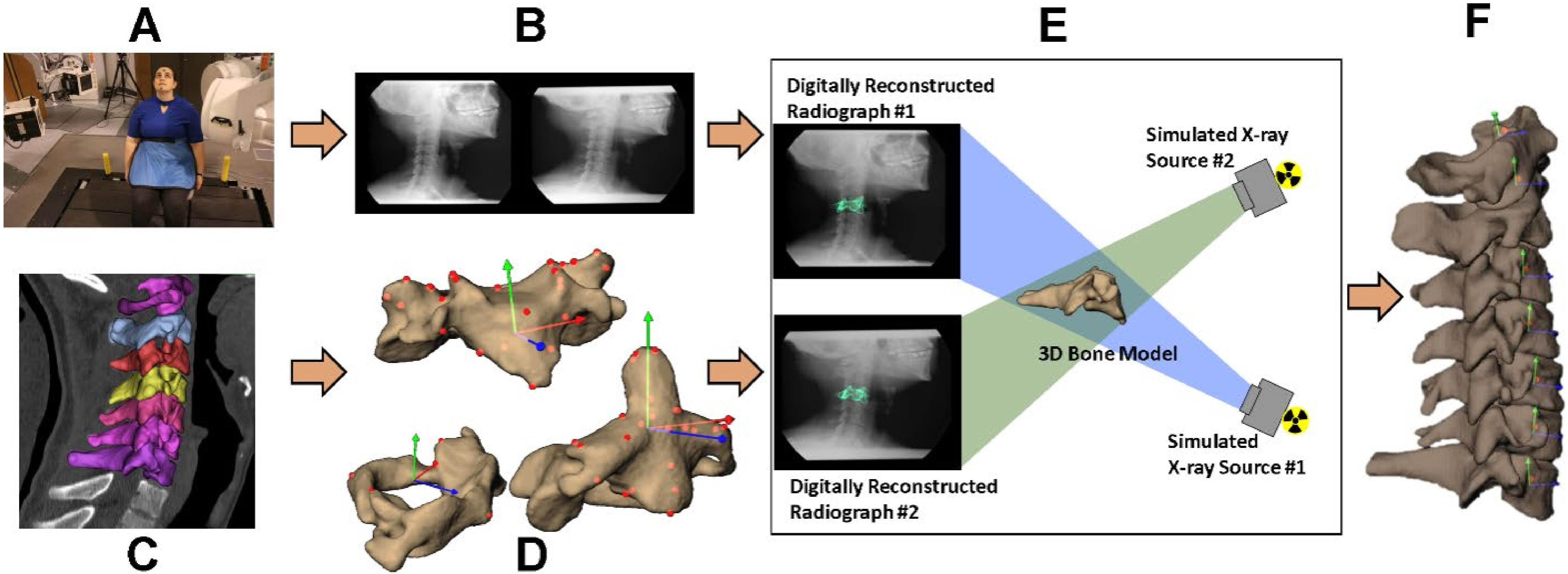

Our collaborators have a unique toolset to **acquire/process the 3D geometry of each vertebra** (C2-C7) from high-resolution CT imaging throughout motion experiments.

Subject-Specific Cervical Spine Geometry

Ligaments: anterior longitudinal ligament (ALL), posterior longitudinal ligament (PLL), interspinous ligament (ISL), ligamentum flavum (LF), capsular ligament (CL) are included; 1-D connector element is used to represent the band structure of ligaments.

Facets: the geometry is based on the subject-specific spine anatomy.

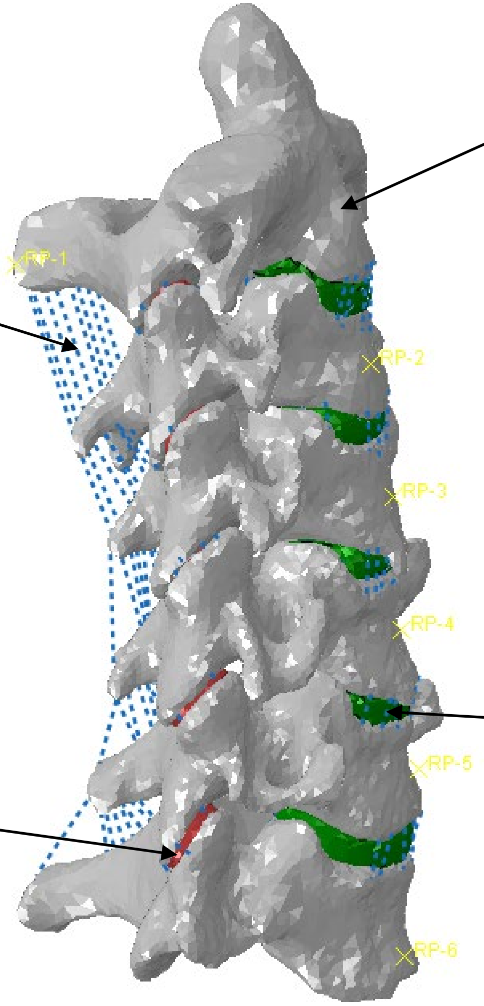

Vertebrae (including **e**nd plates of vertebrae**):**
Rigid bodies (no material property).
(Palomar at al. 2008, Ha 2006)

Intervertebral disc: the geometry of components are based on the subject-specific spine anatomy.

Ligaments

Tension-only nonlinear connectors;
C2-C5 and C5-C7 have distinct properties;
Nonlinear force-displacement relations used:

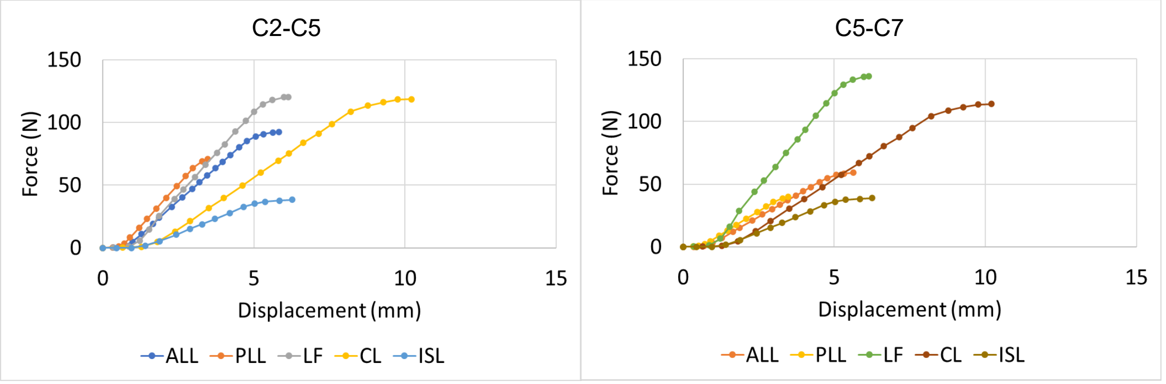

Number of connectors and cross-sectional area specific to type of ligament (size): ALL(6);PLL(5);LF(4);CL(5);ISL(8)

(Chazal et al. 1985; Yoganandan at al. 2000; Panzer and Cronin 2009)

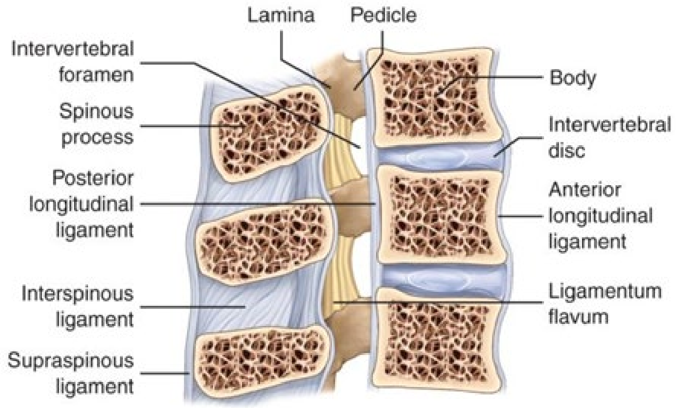

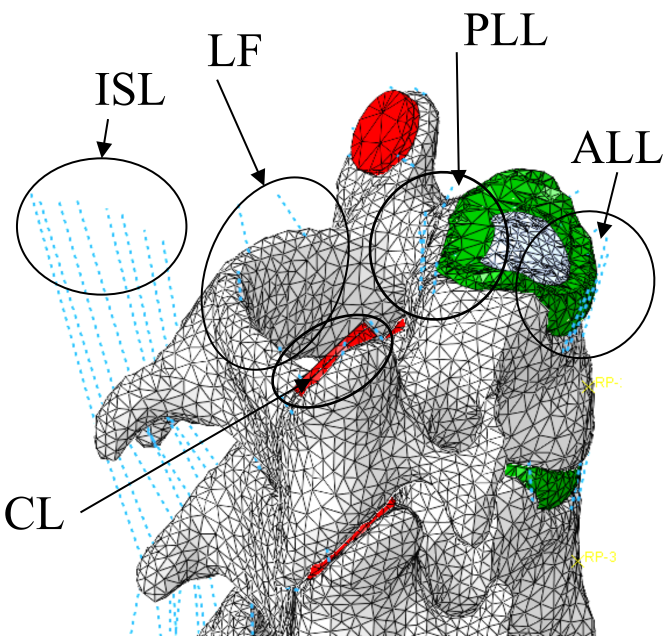

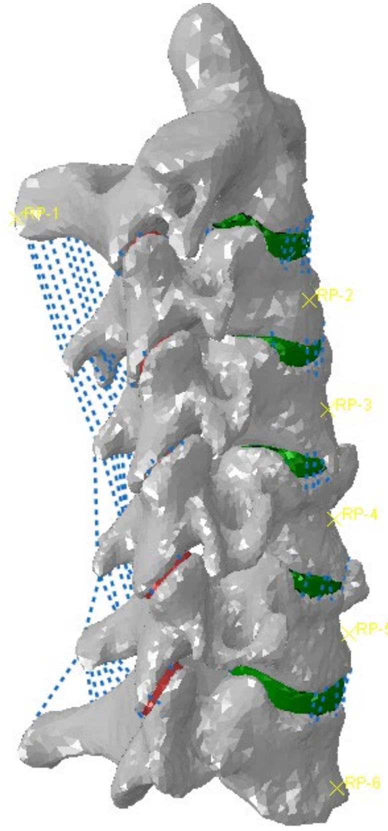

Facet Joints

A facet joint uses two cartilage layers and a frictionless bony gap contact.

Cartilage is linear elastic with E = 10.4 MPa and ν = 0.4.

Pressure-overclosure contact:

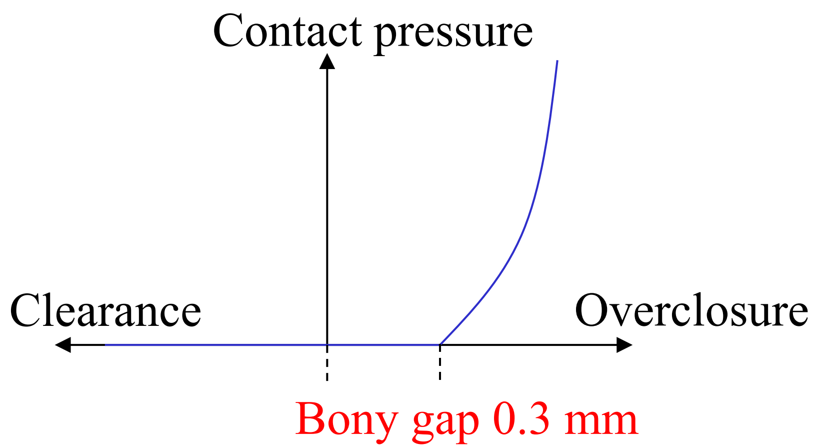

(Mengoni, M. 2021)

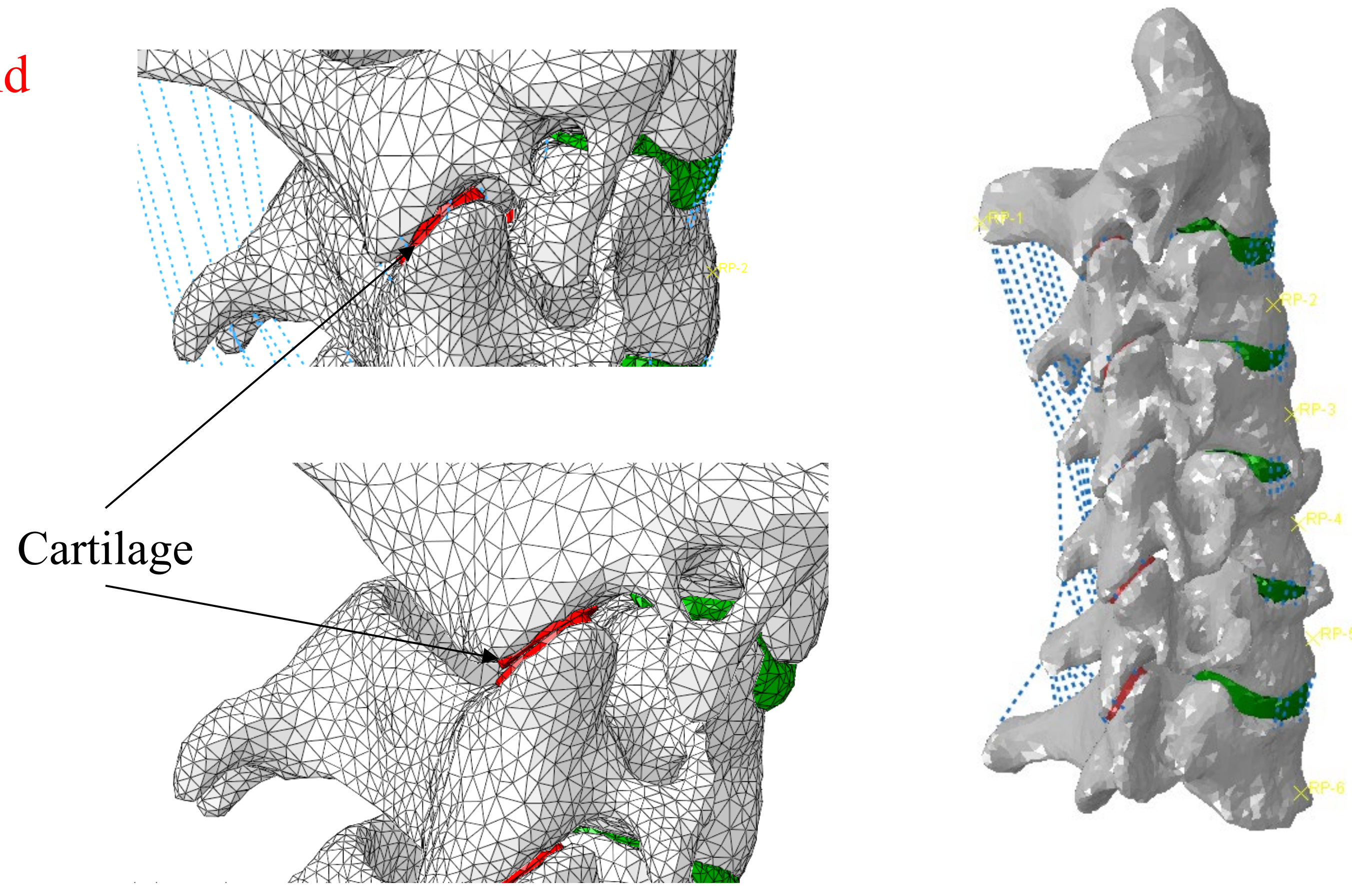

Disc Nuclei and Annulus Ground Substance

Nuclei

Approximately elliptical shape;

Nucleus volume is 40 % - 50 % of the total volume of the disc; *(Pooni 1986)*

Linear elastic material model with E = 2 MPa and ν = 0.49. *(Iatridis 1997; Wang 1997; 2000)*

Annulus Ground Substance

Modeled as a hyper-elastic material: Neo-Hookean solid;

Strain energy density function:

$$U = C_{10}(\bar{I}_1 - 3) + \frac{1}{D_1}(J-1)^2$$

Assumed parameter values (will be calibrated in the following): $C_{10} = 0.133; D_1 = 0.6$ *(wang et al. 2016)*

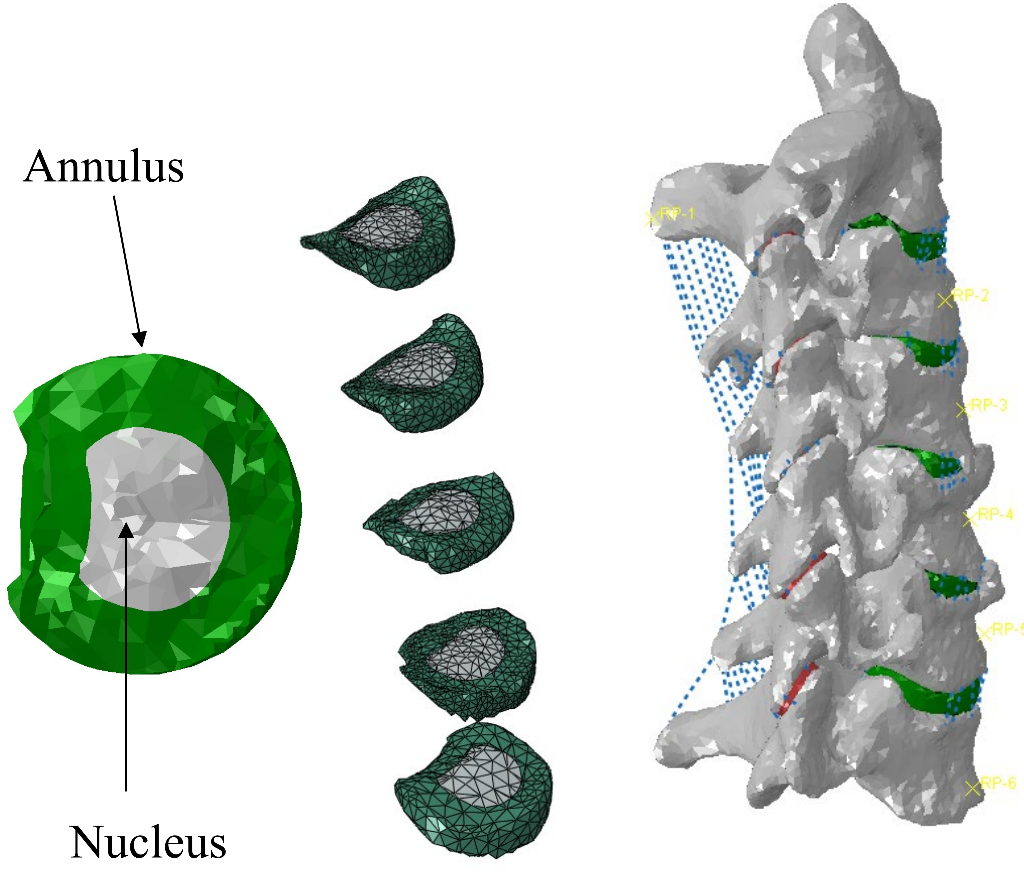

Annular Collagen Fibers (cont.)

Use tension-only nonlinear connectors;

20 connectors in each layer and total volume of two layers of connectors is 19% of the annulus volume;

Nonlinear stress–strain responses of fibers in four anatomical regions of the anulus fibrosus:
Holzapfel et al. (2005)

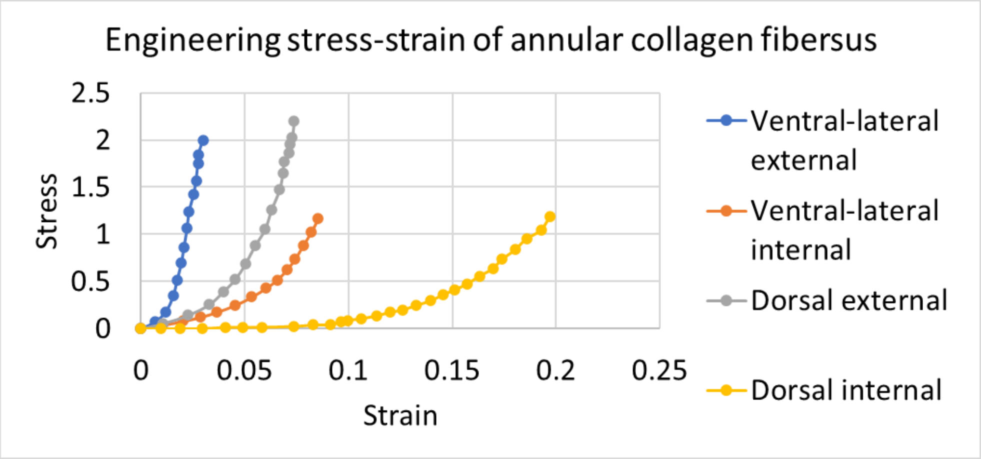

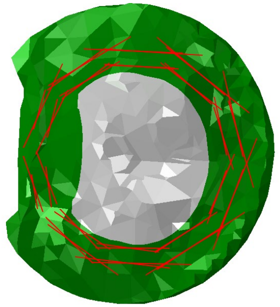

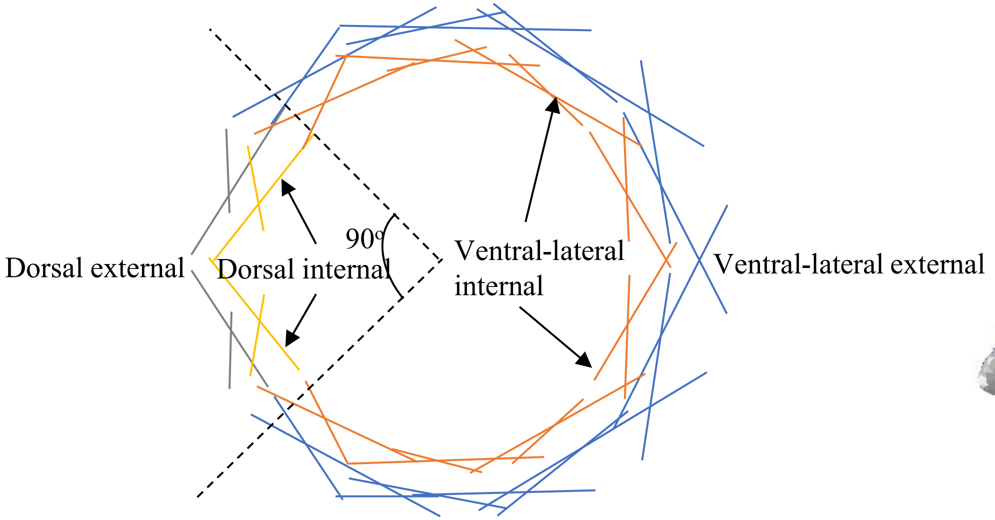

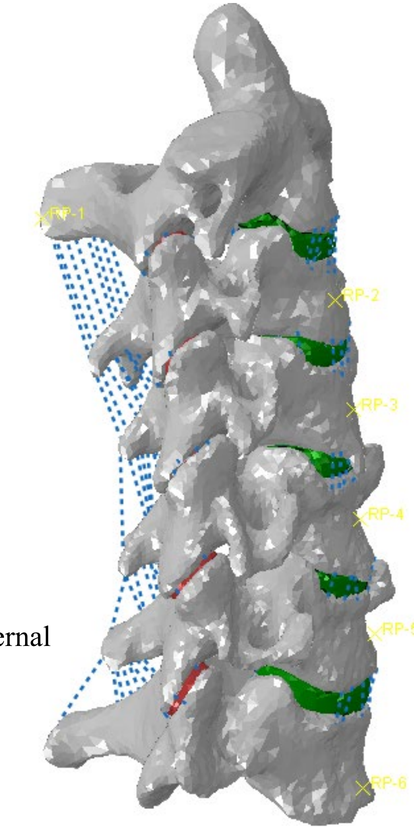

Cadaver Validation

Damping factor: 2×10^{-7}
Mesh number per disc: 4300 – 8600
Annulus ground substance stiffness:
C_{10} **= 0.133 vs. 0.342 vs. 1.1 MPa**

Vertebrae: Rigid body
Annulus ground substance: Hyper-elastic, D_1=0.6 GPa
Nucleus: Elastic, E=2 MPa, v=0.49
Facet: Elastic, E=10.4 Mpa, v=0.4
Ligament: Nonlinear, displacement hardening connector
Annular collagen fiber: Nonlinear, displacement hardening connector
Facet joint contact model: Pressure-overclosure model with 0.3 mm virtual gap, frictionless

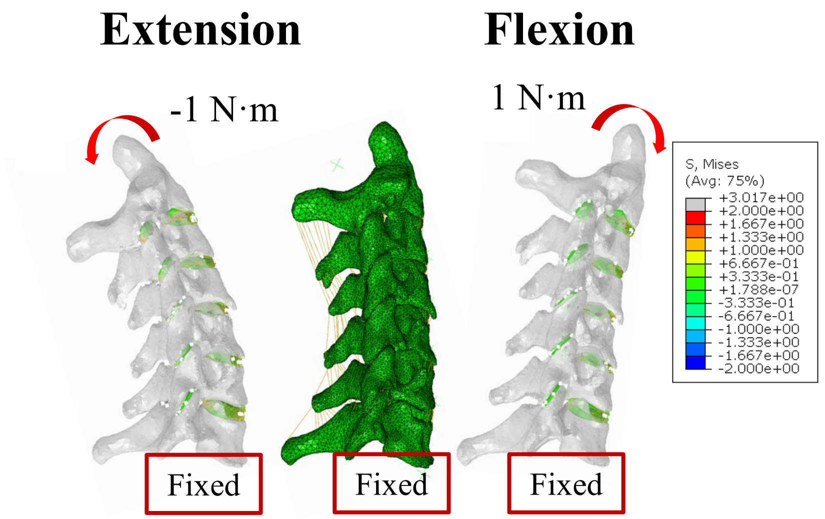

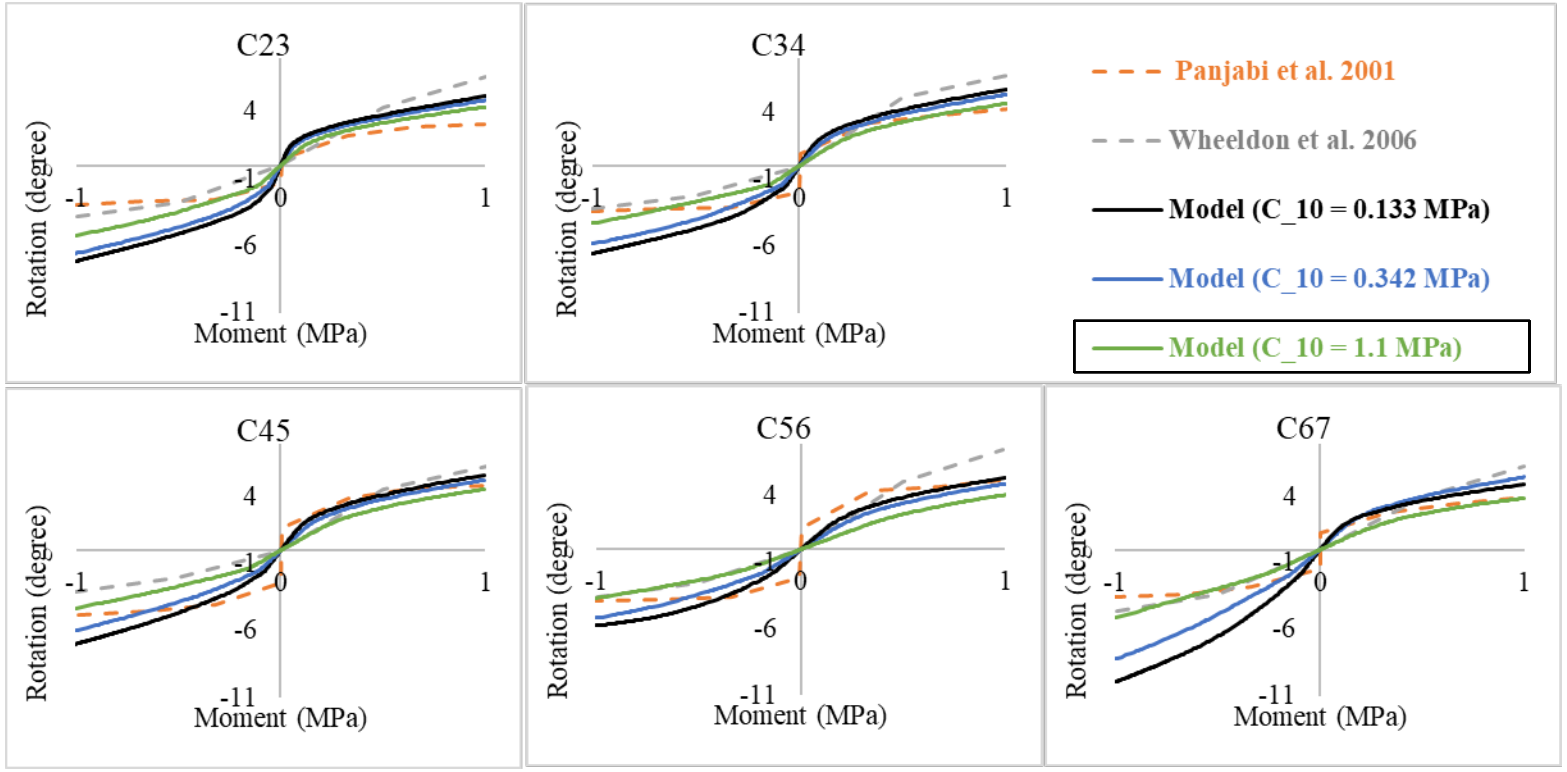

Comparison with *In Vivo* Data

In vivo experimental kinematics

Reference points used for the optimization objective

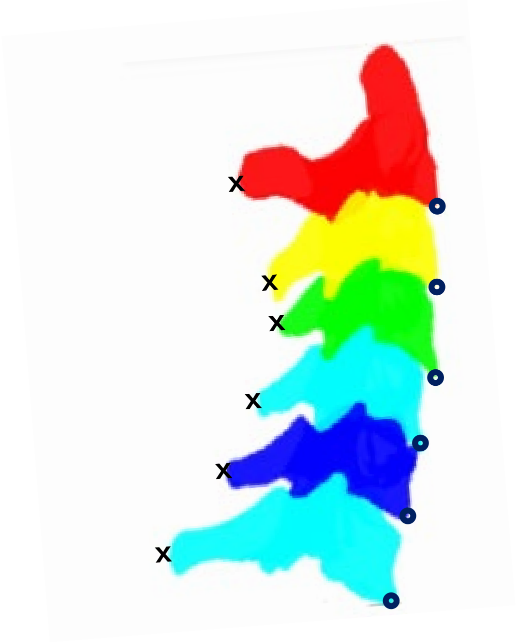

Initial position of reference points

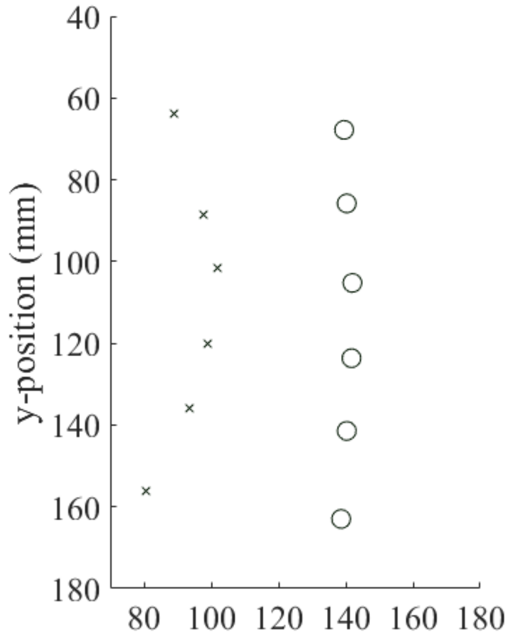

Initial Experimental-Numerical Comparison

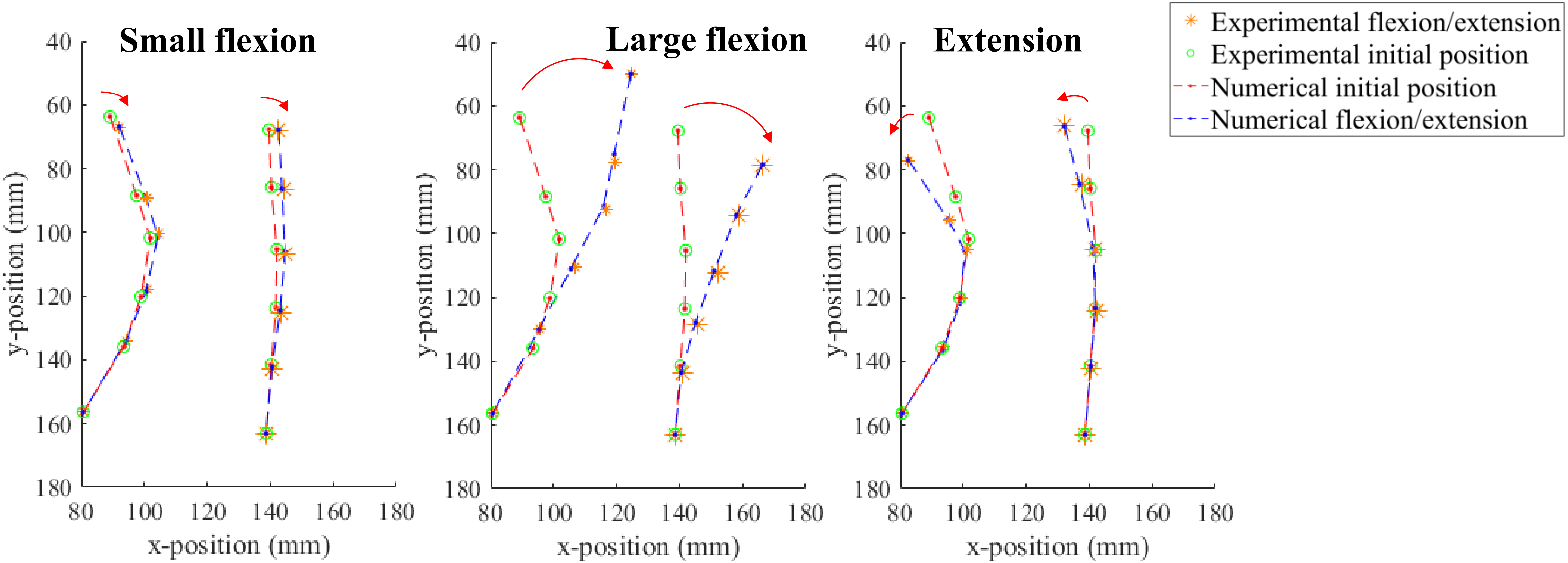

Given $C_{10} = 1.1$ MPa and *in vivo* boundary conditions at C2 and C7, the kinematics of the numerical model diverge somewhat from the *in vivo* flexion/extension data, necessitating some calibration of material properties of each disc.

Inverse Material Estimation (Calibration) Process

Minimization of the objective function

Objective function: $f = \sum_j \sum_i \left\| \boldsymbol{U}_{Rj}^{i} - \boldsymbol{U}_{Ej}^{i} \right\|$

Assumption: Only annulus ground substance is calibrated from our in vivo experimental data, with all other tissues using properties from the literature.

Approach: The material properties are calibrated using a portion of a flexion and extension trial, and then validated using the remaining flexion/extension data.

Initial guess: C_{10}= 1.1 MPa (with min/max = [0.1,10])
Stopping criteria:

$$\|\boldsymbol{C}_{i+1} - \boldsymbol{C}_i\| \leq 10^{-6}$$
$$|f(\boldsymbol{C}_{i+1}) - f(\boldsymbol{C}_i)| \leq 10^{-6}$$

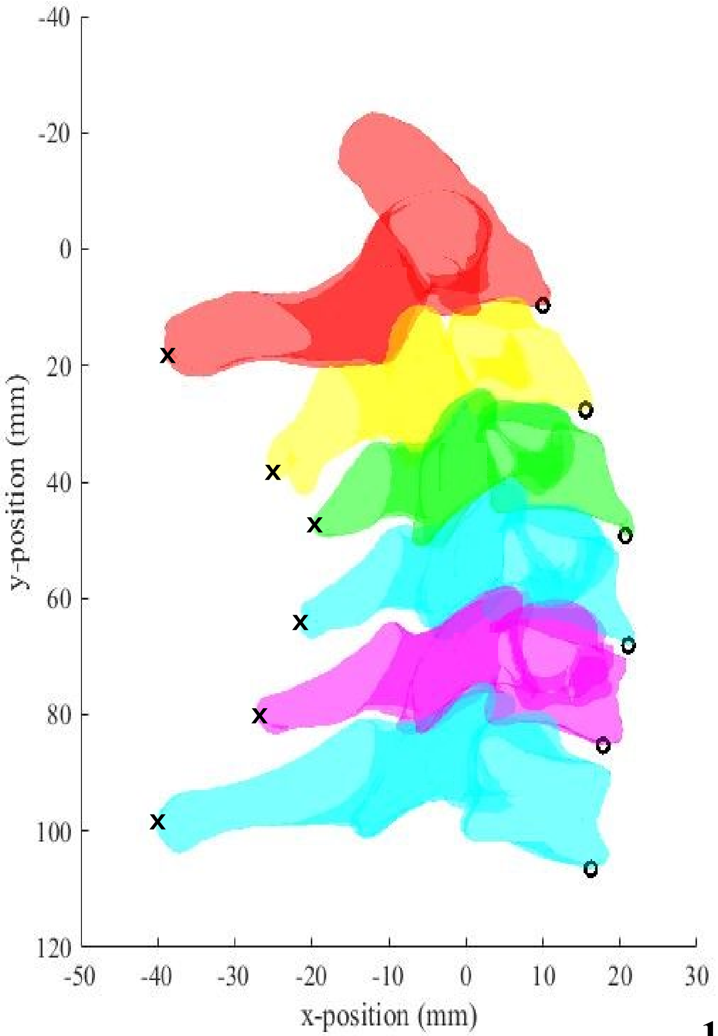

Inverse Material Estimation – Preliminary Results

Initial guess: C_{10}= 1.1 MPa (with min/max = [0.1,10])

Final objective function: $f = 8.45$ mm

Final material property estimate:
$\left[C_{10}^{23}, C_{10}^{34}, C_{10}^{45}, C_{10}^{56}, C_{10}^{67}\right] = [1.1, 0.74, 0.88, 0.32, 0.78]$

Validation:
$Err_{smallFlex} = 3.374$ mm
$Err_{largeFlex} = 3.984$ mm
$Err_{largeExt} = 4.467$ mm
$Err_{smallExt} = 3.097$ mm

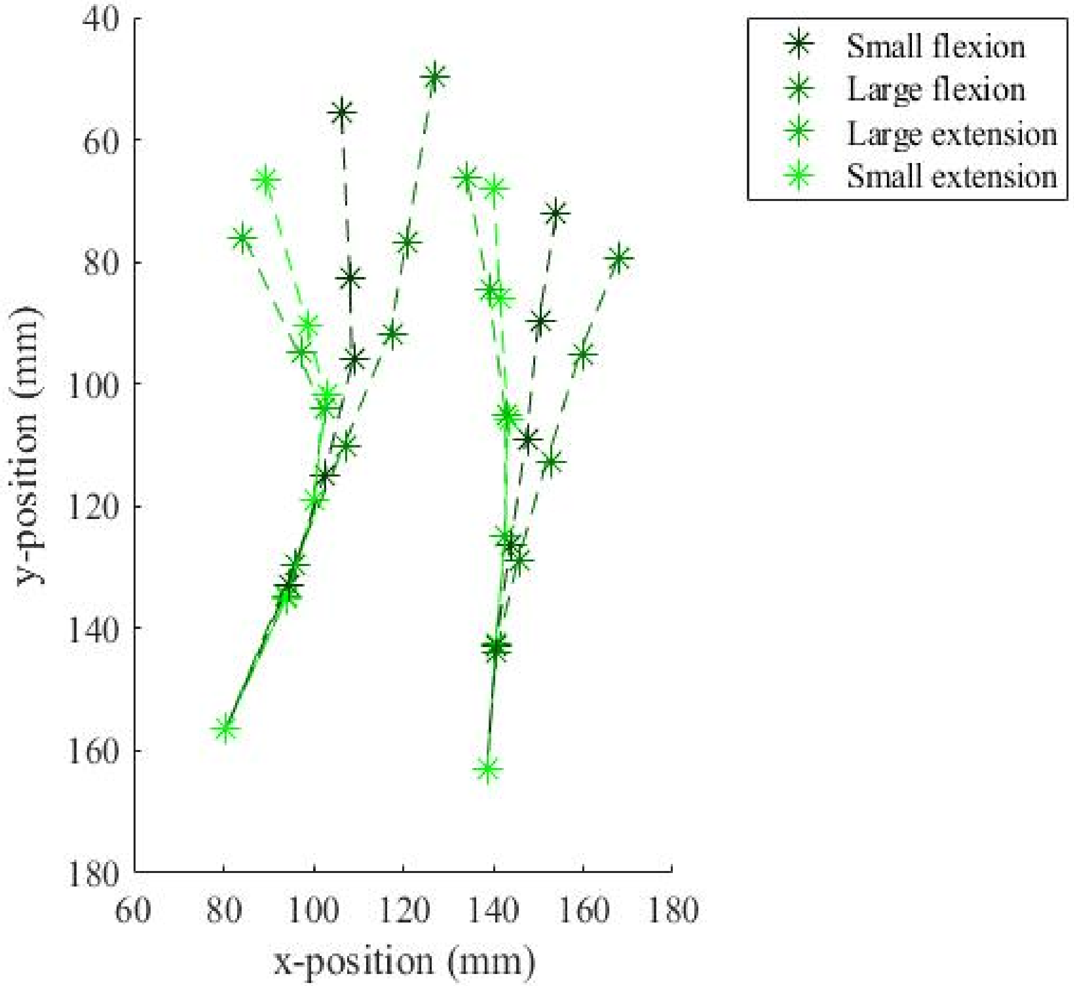

Inverse Material Estimation – Control Subject

Initial guess: C_{10}= 1.1 MPa (with min/max = [0.1,10])

Final objective function: f = 16.20 mm

Final material property estimate:
$[C_{10}^{23}, C_{10}^{34}, C_{10}^{45}, C_{10}^{56}, C_{10}^{67}] = [1.1, 1.08, 0.98, 1.02, 1.03]$

Validation:
$Err_{smallFlex}$ = 4.206 mm
$Err_{largeFlex}$ = 5.488 mm
Err_{Ext} = 10.717 mm

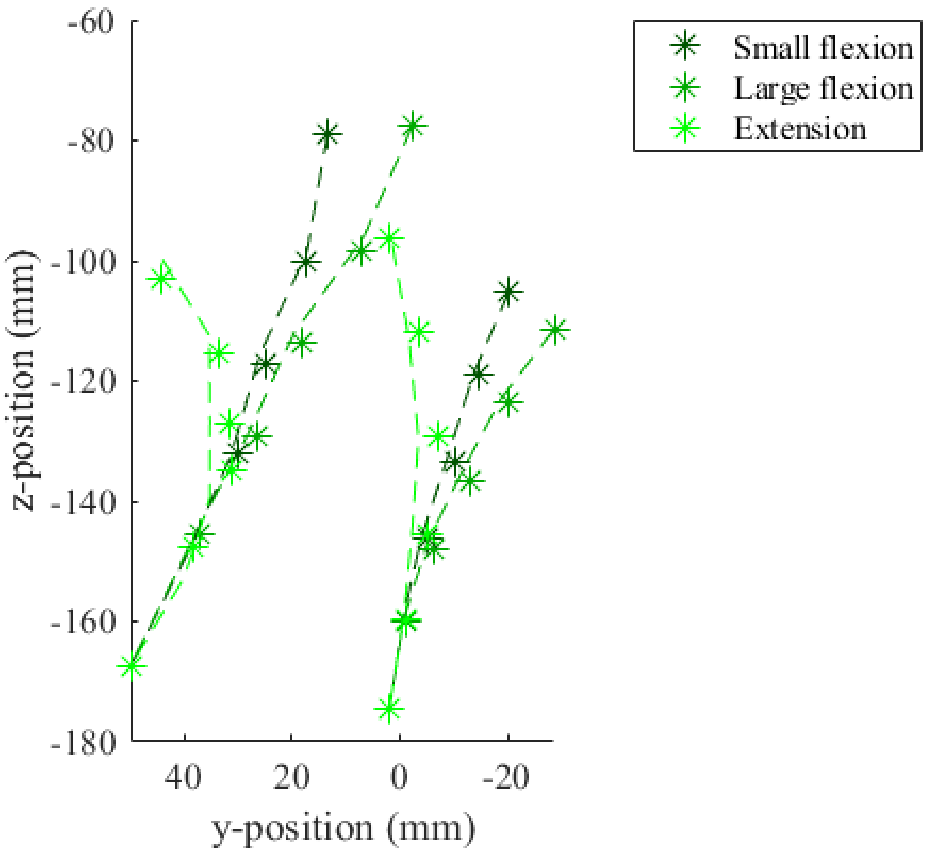

Conclusions and Future Directions

1. A computational approach was established to model subject-specific cervical spines, including realistic geometries from CT imaging and nonlinear tissue properties from the literature.
2. The kinematic behavior of the model was validated through comparison with corresponding results from *in vitro* experiments in the literature.
3. A calibration procedure is proposed to estimate the material properties of each intervertebral disc, by minimizing the difference of kinematics between the numerical model and our *in vivo* experiments.
4. Future work includes:
    a. execution/refinement of the calibration procedure, including consideration of alternate motion trials and loading options.
    b. further upgrading model components/realism and eventually incorporating arthrodesis.

Acknowledgements

- Soumaya Ouhsousou, Clarissa M. LeVasseur, Jeremy Shaw, William Anderst, and John C. Brigham
- Support from the Cervical Spine Research Society (CSRS)

References

- Del Palomar, A. P., Calvo, B., & Doblare, M. (2008). An accurate finite element model of the cervical spine under quasi-static loading. *Journal of biomechanics*, *41*(3), 523-531.
- Ha, S. K. (2006). Finite element modeling of multi-level cervical spinal segments (C3–C6) and biomechanical analysis of an elastomer-type prosthetic disc. *Medical engineering & physics*, *28*(6), 534-541.
- Chazal, J., Tanguy, A., Bourges, M., Gaurel, G., Escande, G., Guillot, M., & Vanneuville, G. (1985). Biomechanical properties of spinal ligaments and a histological study of the supraspinal ligament in traction. Journal of biomechanics, 18(3), 167-176.
- Yoganandan, N., Kumaresan, S., & Pintar, F. A. (2000). Geometric and mechanical properties of human cervical spine ligaments. *J. Biomech. Eng.*, *122*(6), 623-629.
- Panzer, M. B., & Cronin, D. S. (2009). C4–C5 segment finite element model development, validation, and load-sharing investigation. *Journal of biomechanics*, *42*(4), 480-490.
- Mengoni, M. (2021). Biomechanical modelling of the facet joints: a review of methods and validation processes in finite element analysis. *Biomechanics and Modeling in Mechanobiology*, *20*(2), 389-401.
- Pooni, J. S., Hukins, D. W., Harris, P. F., Hilton, R. C., & Davies, K. E. (1986). Comparison of the structure of human intervertebral discs in the cervical, thoracic and lumbar regions of the spine. *Surgical and radiologic anatomy: SRA*, *8*(3), 175-182.
- Iatridis, J. C., Setton, L. A., Weidenbaum, M., & Mow, V. C. (1997). The viscoelastic behavior of the non-degenerate human lumbar nucleus pulposus in shear. *Journal of biomechanics*, *30*(10), 1005-1013.

References

- Wang, J. L., Parnianpour, M., Shirazi-Adl, A., Engin, A. E., Li, S., & Patwardhan, A. (1997). Development and validation of a viscoelastic finite element model of an L2/L3 motion segment. *Theoretical and applied fracture mechanics*, *28*(1), 81-93.
- Wang, J. L., Parnianpour, M., Shirazi-Adl, A., & Engin, A. E. (2000). Viscoelastic finite-element analysis of a lumbar motion segment in combined compression and sagittal flexion: Effect of loading rate. *Spine*, *25*(3), 310-318.
- Wang, Z., Zhao, H., Liu, J. M., Tan, L. W., Liu, P., & Zhao, J. H. (2016). Resection or degeneration of uncovertebral joints altered the segmental kinematics and load-sharing pattern of subaxial cervical spine: A biomechanical investigation using a C2–T1 finite element model. *Journal of biomechanics*, *49*(13), 2854-2862.
- Cassidy, J. J., Hiltner, A., & Baer, E. (1989). Hierarchical structure of the intervertebral disc. *Connective tissue research*, *23*(1), 75-88.
- Shirazi-Adl, A., Ahmed, A. M., & Shrivastava, S. C. (1986). A finite element study of a lumbar motion segment subjected to pure sagittal plane moments. *Journal of biomechanics*, *19*(4), 331-350.
- OHSHIMA, H., TSUJI, H., HIRANO, N., ISHIHARA, H., KATOH, Y., & YAMADA, H. (1989). Water diffusion pathway, swelling pressure, and biomechanical properties of the intervertebral disc during compression load. *Spine*, *14*(11), 1234-1244.
- Holzapfel, G. A., Schulze-Bauer, C. A., Feigl, G., & Regitnig, P. (2005). Single lamellar mechanics of the human lumbar anulus fibrosus. *Biomechanics and modeling in mechanobiology*, *3*, 125-140.